

P. J. Maziasz and T. K. Roche

Metals and Ceramics Division, Oak Ridge National Laboratory  
Oak Ridge, Tennessee 37830

CCAV 810821-11  
MASTER

The first-generation Prime Candidate Alloy (PCA) for the austenitic stainless steel class of alloys for application as a Magnetic Fusion Energy (MFE) first-wall material is a 14 Cr-16 Ni-0.25 Ti modification of type 316 stainless steel. A key parameter for material performance is wall lifetime. The ability of the material to resist swelling and resist embrittlement during irradiation is important to longer wall lifetimes. The microstructure that evolves during irradiation is primarily responsible for both the swelling and embrittlement responses, and helium plays a central role in this microstructural evolution. This paper indicates how preirradiation microstructures that employ control of MC precipitation and dislocation density are designed and produced for fusion application of PCA.

## INTRODUCTION

The effort of the Alloy Development for Irradiation Performance (ADIP) program for Magnetic Fusion Energy (MFE) is divided into several parallel paths for different classes of alloys, each identifying, investigating, and developing a Prime Candidate Alloy (PCA) in that particular class. Austenitic stainless steels (Path A) are leading candidates for early and future devices. The reference material for Path A is 20%-cold-worked type 316 (18 Cr-13 Ni-2 Mo-2 Mn-0.05 C-0.4 Si-bal Fe); the PCA is a 14 Cr-16 Ni-0.25 Ti modification of the 316 type alloy. Several distinct advantages of austenitic alloys are the wealth of irradiation data from a variety of sources, including the Fast Breeder Reactor (FBR) program, compatibility with coolants, fracture toughness, ease of fabricability and welding, and reasonable material costs. Disadvantages include the low thermal conductivity and the long-lived, high level of induced residual radioactivity. A key parameter for material performance is wall lifetime; embrittlement and swelling are important forms of radiation damage that affect this parameter. In addition, these radiation damage responses determine the acceptable neutron wall loading and maximum temperature limit of operation.

Swelling and many mechanical properties changes are directly or indirectly related to the microstructure developed during irradiation. One basic philosophy behind the ADIP program is that controlling the preirradiation microstructure will enable us to control microstructural evolution and property changes during irradiation. Helium plays an important role in microstructural development of type 316 stainless steel during various types of irradiation [1-4]. Increased dislocation density and a fine dispersion of MC precipitate particles are two of the most effective means of controlling helium on a microstructural scale in austenitic alloys [5,6]. This paper summarizes and highlights

the design and development of preirradiation microstructures in PCA based on principles for best controlling the effects of helium.

## MICROSTRUCTURAL DESIGN

The design effort involved examining and evaluating irradiation data on microstructural development, mechanical properties changes and swelling to assess avenues for improving the response of austenitic type alloys to anticipated fusion irradiation conditions [7]. Unlike the FBR or Light Water Reactor (LWR) programs, the MFE program has no engineering facilities to generate data because no fusion reactors actually exist. We rely therefore on examining data from a variety of irradiation environments that include ion facilities, and fast and mixed-spectrum reactors (EBR-11 and HFIR, respectively); the data have been acquired for type 316 and 316 + 0.2 to 0.3 wt % Ti with simple solution-annealed (SA) or 20 to 25%-cold-worked (CW) preirradiation microstructures. In an austenitic stainless steel fusion reactor first wall, helium displacement damage will be generated at a ratio of about 12 to 15 at. ppm He/dpa. Helium plays an important role in microstructural development. Increasing the helium generation rate relating to a fast reactor affects all components of the radiation-induced microstructure [3], indicating a role of helium in many of the basic mechanisms responsible for microstructural evolution. The design effort therefore emphasizes understanding and controlling the effects of helium during irradiation to control the properties.

Increased helium generation in HFIR can either increase or decrease swelling relative to fast reactor irradiation (low helium generation rate) at the temperatures and fluences that characterize the void swelling regime. Helium affects SA or CW materials differently and cavity and precipitation behavior can be intimately co-related

\*Research sponsored by the Office of Fusion Energy, U.S. Department of Energy, under contract No. W-7405-eng-26 with the Union Carbide Corporation.

By acceptance of this article in the publisher or recipient acknowledges the U.S. Government's right to retain a nonexclusive, royalty-free license in and to any copyright covering the article.

## DISCLAIMER

This document contains information that is not to be released to the public, except as may be required by law. It is the property of the U.S. Government and is loaned to you. It and its contents are not to be distributed outside your agency. It is to be destroyed when it is no longer needed. It is to be destroyed when it is no longer needed.

EXEMPT FROM AUTOMATIC DECLASSIFICATION

MGU

in HFIR. Most of the cavities formed in HFIR appear to be bubbles whereas most of the cavities present after FBR irradiation are voids. Even in EBR-II, however, void formation is directly related to earlier bubble formation. Voids are found in some conditions in HFIR, and then the voids will be associated with precipitate particles of  $\epsilon$  or Laves phases, as in fast reactors. Cold working is found to reduce swelling in HFIR by refining the nucleation of cavity structure. However, the initial cold worked dislocation density quickly recovers at temperatures of 285°C and above, and recrystallization makes cold working ineffective above 600–650°C. Swelling is definitely increased for HFIR compared to FBR irradiations at temperatures above and below the void swelling regime. Particularly perplexing is the low-temperature swelling in HFIR that indicates a maximum at around 250°C and appears confined to CW material [8]. Grain boundary cavitation is considerably increased by the increased helium generation rate in HFIR and this leads to both increased swelling and embrittlement. Grain boundary embrittlement resulting from grain boundary cavitation is most responsible for upper limit of about 550–600°C for use of type 316 [9]. Grain boundary cavitation is an important concern for fusion because it is far less controllable in either 316 or 316 + Ti than matrix cavitation, and it is very temperature sensitive, increasing dramatically with increasing temperature.

After considering the effects of helium, it is easy to appreciate the benefits of the MC interfacial helium trapping to alloy development of austenitic stainless steels for fusion application (see Fig. 1). MC particles apparently gather nearly all of the helium generated in

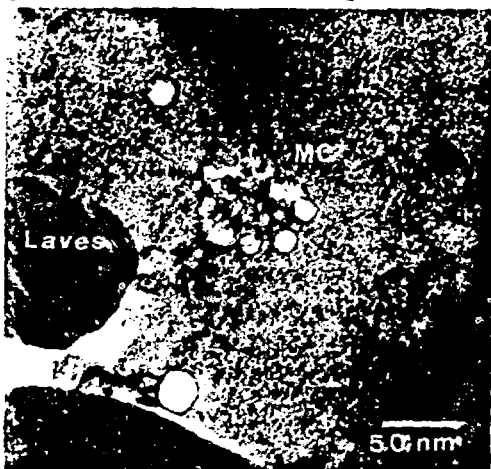


Fig. 1. An example of MC interfacial helium trapping in SA 316 + Ti irradiated in HFIR at 600°C to 1850 at. ppm He and 30 dpa.

the surrounding matrix during irradiation to form a fine and concentrated dispersion of bubbles at or near the interface. The underlying reasons involve the oversize misfit of the MC phase that allows it to collect and absorb vacancies during particle growth, which, in turn, somehow drag helium with them [6]. This effect is observed for MC and helium under a wide variety of irradiation conditions. In CW 316 + Ti, the MC precipitation and increased dislocation density are mutually beneficial. The dislocation density refines the scale of MC precipitation relative to SA material and the MC particles in turn pin the dislocation structure [3]. MC formation also coincides with reduction or elimination of precipitate phases like gamma prime,  $\epsilon$ , tau, Laves and G-phases [10,11]. Identification, characterization, and evaluation of these phases indicate they are either associated with void swelling or else offer no apparent benefit. Several of these phases can interfere with MC stability or formation through competition for solutes like Mo, Ti, or C, also making them undesirable.

The microstructural design effort for the PCA therefore identified preirradiation microstructures that would encourage effects most beneficial for controlling helium. SA, 10 and 25% CW microstructures were chosen to vary dislocation concentration without any superimposed precipitation effects. Both the effects of helium on phase stability (more thermal rather than radiation induced phases during irradiation) and the fact that irradiation often produces phases with compositions similar to their thermal counterparts (particularly for MC) [3,6,10,11] make the development of preirradiation microstructures with stable thermal phases quite relevant to irradiation application. Other preirradiation microstructures were therefore envisioned that would vary MC precipitate size and spatial distribution together with varying the dislocation concentration in the matrix. It was thought quite important to encourage MC formation and stability at the grain boundaries, because of its interfacial helium trapping behavior. MC is not the normal or sole grain boundary phase observed during thermal aging of either modified or unmodified austenites with compositions close to type 316. To make matters worse, the grain boundary phases that do form naturally in these alloys – namely  $\epsilon$ , Laves and tau phases – tend to dissolve or do not form at all during HFIR irradiation at about 500–550°C and above, leaving the grain boundaries open to helium cavity formation.

#### MICROSTRUCTURAL DEVELOPMENT AND PRODUCTION

About 0.2 to 0.3 wt % Ti has been shown to be an optimum concentration, for several different alloys considering several different properties [12,13]. PCA is adjusted in nickel and chromium from type 316 (as mentioned earlier) primarily for reduced susceptibility to sigma phase

formation. A 1.4 Mg (3000 lb) heat was double vacuum melted from virgin materials and fabricated from ingot to plate and bar stock by the vendor. The objective was to fabricate as-received vendor stock to finished product (primarily sheet) with designed microstructures. The as-received material contained stringers of MC carbide and an inhomogeneous titanium concentration in the matrix. MC stringering is common in many reactive or refractory metal-modified alloys [14]. Stringers were eliminated by high-temperature homogenization for 24 h at 1275°C. In addition, a detailed investigation of the sensitivity of homogeneity and microstructures to fabrication variables was conducted to determine fabrication routes that would not re-introduce MC stringering or inhomogeneity [15-18]. Microstructures were monitored at various stages by both metallography and transmission electron microscopy (TEM). It was found most important to be aware of MC precipitation occurring during processing. Scheduling short homogenizations of about 1 h at 1200°C after several processing steps helped keep the homogeneity intact and prevented extensive MC stringering.

TiN formed near the surface of the homogeneous, MC-free material during heat treatment in air. TiN is very stable and its presence caused a duplex grain structure to develop in the surface region. This difficulty was eliminated by conducting all heat treatments in vacuum or an inert gas atmosphere.

Isothermal time-temperature-precipitation (TTP) response of SA, and 10 and 25% CW material was determined using TEM. This determination also revealed how the microstructures varied with thermal-mechanical treatment (TMT) [16]. These studies revealed the single or multiple step TMTs necessary to produce the design microstructures at the end of the fabrication sequence. Homogeneity and absence of MC stringers are essential to successful microstructural manipulation, but the high-temperature heat treatments that give best results also make the grain size rather large. It was therefore important to also manipulate grain size without interfering with the precipitate microstructures. The TTP curves revealed that recrystallization could be uncoupled from the MC precipitation phenomena to accomplish this.

The isothermal aging studies from 650 to 1100°C demonstrate that PCA is much more phase-stable than either type 316 or 316 + Ti stainless steels. The titanium-rich MC carbide is the primary precipitate phase. Small amounts of Laves phase can be observed in 25% CW PCA after 166 h at 750°C. However, sigma, chi, eta and tau phases are definitely not observed, as in 316 or 316 + Ti [3,11]. Longer term aging is necessary to determine whether chi and sigma phases will form, but these times and temperatures indicate resistance to eta, tau and Laves phase formation. PCA with 14 Cr-16 Ni is definitely superior to 316 + Ti with 18 Cr-12 Ni because the stable grain

boundary phase is MC rather than the mix of tau, eta and Laves phase observed in 316 + Ti [11]. MC was identified as desirable at the grain boundary in the microstructural design section because of its helium trapping behavior.

The first portions of alloy design and development — namely, control of undesirable phase instability and formation of MC both at the grain boundaries and in the matrix — were achieved as a result of changes in matrix chemistry of PCA compared to a normal 316 alloy. The second portion of alloy design — to vary the size distribution and spatial dispersion of matrix and grain boundary MC — was accomplished by combining the TEM microstructural information together with the TTP information for SA and 10 or 25% CW material.

The microstructurally determined TTP curves revealed that MC precipitation is very rapid in 10 or 25% CW materials. We will describe the precipitation results most important to producing the design microstructures. The MC precipitate is very fine, consisting of about  $2-5 \times 10^{22}$  particles/m<sup>3</sup> that are about 3-5 nm in size and uniformly dispersed along the network of dislocation lines [17,18]. In CW material, grain boundary MC is as fine as in the matrix. Both precipitate size and dispersions are temperature insensitive in CW material from 650 to 900°C, until recrystallization occurs. In SA material, MC precipitation is much coarser than in CW material, both in the matrix and at the grain boundary. The precipitation kinetics in SA material are much slower than in CW material. MC precipitation takes from 10 min to several hours to occur at 800 to 950°C. Grain boundary precipitation occurs first and the matrix precipitation occurs hours afterwards. Both size and dispersion of matrix and grain boundary MC are sensitive to aging temperature in SA material, in contrast to the temperature independent behavior in CW material. Together these facts about microstructure, time and temperature reveal how cold working, solution annealing, and various aging treatments could be combined to manipulate MC in the preirradiation microstructure.

The microstructures developed are listed and described in Table 1. Table 2 lists the thermal-mechanical treatments required to produce them. Complete fabrication flowcharts and both metallography and TEM of the final material are included elsewhere [17,18]. Preirradiation microstructures A1, A2, and A3 are produced simply by solution annealing, 10 and 25% cold working homogenized material, respectively. Intercomparison of these samples will give the effect of cold work and hence initial matrix dislocation concentration on properties and serve as a base line for microstructures that develop MC precipitation before irradiation. A3 gives a direct comparison with the standard reference material, 20 to 25% CW 316. Microstructure C is produced by a simple heat treatment of 2 h at 750°C of 25% CW material to

Table 1. Proposed Preirradiation Microstructures That Can Be Achieved by Thermal-Mechanical Treatment of the Prime Candidate Alloy (PCA)

- A. Simple microstructures resulting from:
  1. solution annealing,
  2. 5 to 10% cold working, or
  3. 20 to 25% cold working.
- B. Microstructures with both coarse grain boundary MC precipitation and intragranular MC precipitation consisting of:
  1. coarse particles or particle clusters or
  2. fine matrix precipitation.
- C. Microstructures with both fine grain boundary MC precipitation and fine intragranular MC matrix precipitation.
- D. Microstructures with both fine grain boundary MC precipitation and fine intragranular MC matrix precipitation plus increased dislocation density.

produce the fine MC in the matrix and at the grain boundaries. Comparison of A3 and C indicates the effect of producing fine MC everywhere in heavily cold-worked material prior to irradiation.

The remaining preirradiation microstructures are either innovative microstructures with special features designed for the fusion environment or microstructures that involve multistep processing. Microstructure B1 is basically a solution-annealed dislocation density with coarse MC precipitation developed at the grain boundaries and in the matrix. TEM plus the TTP curve for SA material indicate that optimum distributions of both MC components are not developed by isothermal treatment at a single temperature. However, the TTP for SA material revealed that the desired grain boundary MC precipitate could be developed before MC occurs in the matrix. The grain boundary MC was developed by aging for 8 h at 800°C and the matrix MC was then produced by aging for 8 h at 900°C [7].

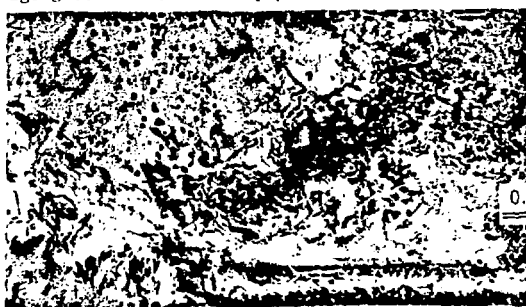


Table 2. Recommended Thermal-Mechanical Treatments to Produce Proposed Preirradiation Microstructures

Micro-structure <sup>a</sup>	Initial Suggested Thermal-Mechanical Treatment
A1	25% cold worked plus 15 min at 1175°C
A2	15 min at 1175°C plus 10% cold worked
A3	15 min at 1175°C plus 25% cold worked
B1	Solution annealed plus 8 h at 800°C plus 8 h at 900°C
B2	Solution annealed plus 8 h at 800°C plus 25% cold worked plus 2 h at 750°C
C	25% cold worked plus 2 h at 750°C
D	10% cold worked plus 2 h at 750°C plus 10% cold worked

<sup>a</sup>Letter and number codes refer to microstructures defined in Table 1.

Microstructures B2 and D do not occur naturally in simply aged SA or CW material. They do, however, result from combining information from TEM and from several TTP curves. Their successful production demonstrates the importance of understanding the principles of microstructural development during processing. Microstructure B2 has the same fine matrix MC as microstructure C. However, B2 has the same coarse grain boundary MC as developed in B1. Microstructure B2 is shown in Fig. 2. It was developed by aging SA material for 8 h at 800°C and then cold working the sheet to a 25% reduction in thickness and finally aging again for 2 h at 750°C. Comparison of B2 with C will indicate the effect of changing the initial grain boundary MC distribution while holding the matrix MC distribution constant. Comparing B2 with B1 varies matrix MC while holding the grain boundary distribution constant. B2 is important because precipitate dissolution during neutron irradiation is possible [3,10], even for MC, and it is



Fig. 2. An example of coarse grain boundary and fine matrix MC for the innovative microstructure of B2 (Table 2) in PCA using (a) bright field and (b) precipitate dark field of the same area.

thought that the coarser grain boundary MC produced at higher temperatures could be more stable. Helium trapping depends on MC stability.

Microstructure D is an attempt to both increase dislocation density and stabilize it against recovery. It is well known that dislocation structures produced by cold deformation usually have a cellular texture on a fine scale with regions of low concentration surrounded by walls of very dense tangles. The dislocation density and structure saturate at some point with increasing cold work level because recovery will balance new dislocation generation. The idea was to obtain a near-saturation structure by cold working 10%. The material was then heat treated for 2 h at 750°C to produce fine MC to pin this dislocation structure. The material was then cold worked an additional 10% and microstructurally the dislocation cell walls became very thick and the cell interiors began to fill in unlike the structures produced by normal cold working at levels up to 50% (this is shown in detail elsewhere [18]). This microstructure has a very high dislocation density, and with the fine MC, is suspected to be more resistant to recovery than normal heavily cold-worked material.

The final portion of alloy design was to manipulate grain size independent of the MC precipitate microstructures. The key to this goal was causing the recrystallization kinetics to be about the same or faster than the MC precipitation kinetics [18]. This is nontrivial because MC can form in less than 2 min at 750 to 850°C.

In homogenized material without precipitation, grain size is a function of annealing temperatures, increasing as the annealing temperature increases. The solution annealing temperature for the first set of preirradiation microstructures described above was 1175°C (for 15 min) and this yielded a coarse grain size of ASTM 1-3. The principle of achieving uniform grain size was to achieve a high, continuous heating rate up until at least 900-1000°C to avoid the nose of the TTP curve for MC precipitation in CW material. Grain size was then simply set by choosing the final annealing temperature and time (0.5 to 1 h). In addition, the kinetics of recrystallization were maximized by keeping the final cold work level prior to recrystallization at 40-50%. These same steps were applied with a final annealing temperature of 1100°C instead of 1175°C, and the grain size was uniformly refined to ASTM 7-8 [18]. A small amount of MC was introduced in the solution-annealed material with refined grain size, but the microstructures listed in Tables 1 and 2 were still successfully produced with little perturbation.

The above efforts, designated Phase I, complete the design and development of preirradiation microstructures in the first-generation PCA. Phase II of alloy development for austenitic stainless steels will involve various irradiation

and testing to evaluate the results of Phase I. Ongoing evaluation includes irradiation in the Oak Ridge Research Reactor (ORR) and in HFIR, as well as long-term thermal aging. Various types of unirradiated and postirradiated mechanical properties and microstructural examination are planned. This work emphasizes combining materials science and physical metallurgy to design and successfully produce preirradiation microstructures for fusion applications. The organization of effort into the several interrelated and sequential phases demonstrates that a systematic approach rather than serendipity is the foundation for producing the best candidate that Path A can offer.

#### REFERENCES

- [1] K. Farrell, *Rad. Effects* 53 (1980) 175-194.
- [2] J. A. Spitznagel, F. W. Wiffen, and F. V. Nolfi, *J. Nucl. Mater.* 85&86 (1979) 629-646.
- [3] P. J. Maziasz, J. A. Horak, and B. L. Cox, to be published in *Proc. Symp. Irradiation Effects in Fusion Stability*, eds., J. R. Holland, L. K. Mansur, and D. I. Potter, TMS/AIME (1981).
- [4] E. A. Kenik and E. H. Lee, *ibid.*
- [5] P. J. Maziasz, F. W. Wiffen, and E. E. Bloom, *Proc. Intern. Conf. on Radiation Effects and Tritium Technology for Fusion Reactors*, CONF-750989, Vol. 1 (March 1976), pp. 259-288.
- [6] P. J. Maziasz, *ibid.*, ref. [3].
- [7] P. J. Maziasz, *ADIF Quart. Progr. Rept.* June 30, 1979, DOE/ET-0058/6, pp. 48-56.
- [8] P. J. Maziasz and M. L. Grossbeck, elsewhere, this publication.
- [9] E. E. Bloom et al., *Nucl. Technol.* 31 (1976) 115-122.
- [10] E. H. Lee, P. J. Maziasz, and A. F. Rowcliffe, *ibid.*, ref. [3].
- [11] P. J. Maziasz, *ADIF Quart. Progr. Rept.* June 30, 1980, DOE/ER-0045/3, pp. 75-129.
- [12] E. E. Bloom, J. M. Leitnaker, and J. O. Stiegler, *Nucl. Technol.* 31 (1976) 232-243.
- [13] E. E. Bloom and J. R. Weir, Jr., *Irradiation Effects in Structural Alloys for Thermal and Fast Reactors*, ASTM-STP-457 (1969), pp. 261-289.
- [14] D. N. Braski and J. M. Leitnaker, *Met. Trans.* 10A (1979) 427-432.
- [15] P. J. Maziasz and T. K. Roche, *ADIF Quart. Progr. Rept. Sept. 30, 1979*, DOE/EP-0058/7, pp. 83-102.
- [16] P. J. Maziasz et al., *ibid.*, pp. 103-127.
- [17] P. J. Maziasz et al., *ADIF Quart. Progr. Rept. March 31, 1980*, DOE/ER-0045/2, pp. 20-32.
- [18] P. J. Maziasz and T. K. Roche, *ADIF Quart. Progr. Rept. Dec. 31, 1980*, DOE/ER-0045/5, pp. 25-42.